Available online at www.sciencedirect.com
SCIENCE DIRECT
ELSEVIER
European Journal of Mechanics A/Solids 24 (2005) 23–33
EUROPEAN JOURNAL OF MECHANICS A/SOLIDS

A one-dimensional model for blood flow in prestressed vessels

Paola Nardinocchi [a,*], Giuseppe Pontrelli [b], Luciano Teresi [c]

[a] *Dipartimento di Ingegneria Strutturale e Geotecnica, Università degli Studi di Roma "La Sapienza", via Eudossiana 18, 00184 Roma, Italy*
[b] *Istituto per le Applicazioni del Calcolo, CNR, Viale del Policlinico 137, 00161, Roma, Italy*
[c] *Dipartimento di Strutture, Università "Roma Tre", Via Vito Volterra 62, 00146, Roma, Italy*

Received 28 November 2003; accepted 15 October 2004

Available online 13 December 2004

Abstract

We are interested in developing a simple model to investigate blood–vessel interactions in a finite arterial segment of the cardiovascular tree. For this purpose, we developed a continuum model for a vascular segment, and we coupled it with a discrete model for the remaining systemic circulation. In working out the modeling, we addressed some main issues, such as the nonlinearity of blood flow, the compliance of the vessel and the prestress state of the artery walls, that is always present aside from the filling of blood. Moreover, we set a discrete model capable of providing appropriate boundary conditions to the continuum model, by reproducing the proper waveforms entering the vessel and avoiding spurious reflections.

Keywords: Blood–wall interaction; Prestressed vessels; Arterial flow

1. Introduction

Our aim is to develop a simple model to investigate blood–vessel interactions in a finite arterial segment of the cardiovascular tree in such way to take into account high stress to which the artery walls are subjected at physiological conditions.

Arterial walls are involved in growth and remodelling phenomena for the adaption to changes with physiological conditions due to ageing or pathological processes. As evidenced by many experiments and measurements (see Fung, 1993; Zhou and Fung, 1997), the most evident mechanical consequence of such phenomena is the presence in arterial walls of high residual stress states, both in circumferential and longitudinal directions (aside form the presence of the blood flowing within the vessel). Thus, the actions exerted by the fluid on the vessels walls yield a stress state that is added onto an existing stress field. This evidence has produced in the past years scientific literature aimed at providing appropriate constitutive recipies for the artery walls (see Holzapfel et al., 2000; Holzapfel and Ogden, 2003), and at describing the mechanical behaviour of prestressed compliance vessels filled with viscous incompressible fluid (see Atabek and Lew, 1966; Kuiken, 1984; Nardinocchi and Teresi, 2003).

In addition to what has been said, the complexity of the phenomena related to the blood–vessel interaction, due to the fairly intricate mechanical characteristics of blood vessels, and to the different time and space scales at which different but related phenomena occur, have created a wide spread of models having different levels of descriptive capability (see Quarteroni, 2001; Quarteroni and Formaggia, 2003; Formaggia et al., 1999; Sherwin et al., 2003; Di Carlo et al., 1999; Pontrelli, 2000).

* Corresponding author.
E-mail addresses: paola.nardinocchi@uniroma1.it (P. Nardinocchi), g.pontrelli@iac.cnr.it (G. Pontrelli), teresi@uniroma3.it (L. Teresi).

0997-7538/$ – see front matter
doi:10.1016/j.euromechsol.2004.10.002

The idea we are following here is to develop a simple continuum model for a compliant cardiovascular district, having a straight cylindrical configuration and no branchings; encompassing both blood flow and vessel displacement, and to couple it with a discrete model for the remaining systemic circulation. In particular, we model the blood as an incompressible, linearly viscous fluid, whose behaviour is described by a cross-average equation derived from the full 3D balance equations, plus the incompressibility constraint. Then, providing that for the present study the bending stiffness of the arterial walls be negligible, we model the vessel as an axisymmetric membrane whose response can be predicted by assigning a strain-energy function properly tuned to mimic load-test results, and investigate its mechanical behaviour due to small deformations superimposed on finite deformations. The latter, having the role of independent parameters, account for the stresses present in the in vivo arteries, whereas the superimposed deformations account for the small effects due to the pulsatile blood pressure, as proposed in Nardinocchi and Teresi (2003).

It is worth noting that in order to match the fluid and the solid descriptions and, in contrast with the standard usages in fluid mechanics, we describe the fluid flow in a referential form (Di Carlo et al., 1999).

Finally, we set a discrete model that provides a rougher description of the flow variables (Pontrelli, 2004), and is able to yield appropriate boundary conditions to the continuum, by reproducing the proper waveforms entering the vessel and avoiding spurious reflections.

Eventually, we must tackle a system composed of four partial differential equations, describing pressure and flow velocity, and the vessel's wall displacements, defined at a time interval multiplied by a (one-dimensional) space interval, coupled with a system of time dependent ordinary differential equations describing the remaining systemic circulation. This problem has been solved via numerical techniques for a given range of initial conditions and prestress parameters. The results are collected and discussed.

2. Vascular district modeling

Our aim is to describe blood flow in large arteries in the framework of a fluid-solid interaction problem. In the study under consideration, the blood behaviour is that of an incompressible, linearly viscous fluid, whereas the bending stiffness of the vessel wall is so small that prompts us to use an axisymmetric elastic membrane for modeling it.

We model here a single tube-like vascular district; more precisely, let us denote with $\mathcal{E}$ the three-dimensional Euclidean space and with $\mathcal{V}$ the associated translation space. Then, given an orthonormal Cartesian frame with origin $o \in \mathcal{E}$ and basis $\mathbf{i}_\alpha \in \mathcal{V}$ $(\alpha = 1, 2, 3)$, we consider a cylindrical region Ω, with axis parallel to $\mathbf{e} = \mathbf{i}_1$ and having as cross section an open disk $\mathcal{L}$ centered at o; in terms of cylindrical coordinates (s, α, ϱ), the cylinder Ω is the set of points $p \in \mathcal{E}$ given by

$$\Omega = \big\{ p = p(s, \alpha, \varrho) = o + s\mathbf{e} + \varrho\mathbf{c}(\alpha),\ s \in \mathcal{I},\ \alpha \in (0, 2\pi),\ \varrho \in (0, R) \big\}, \tag{1}$$

where $\mathcal{I} = (0, L)$ parametrizes the cylinder axis and $\mathbf{c}(\alpha) = \cos\alpha\mathbf{i}_2 + \sin\alpha\mathbf{i}_3$ is the unit vector spanning the cross section.

The blood is modelled as a three-dimensional continuum whose kinematical and dynamical descriptors are defined on the interior of Ω; the vessel wall is modelled as a membrane whose reference configuration is the surface of the cylinder Ω. At time t, the current configuration $\mathcal{C}$ of the membrane is described through the fields x, r from $\mathcal{I} \times \mathcal{R}$ onto $\mathcal{R}$ as

$$\mathcal{C} = \big\{ o + x(s, t)\mathbf{e} + r(s, t)\mathbf{c}(\alpha), s \in \mathcal{I}, \alpha \in (0, 2\pi) \big\}, \tag{2}$$

or, alternatively, through the fields u, w denoting the axial and the radial displacement of the membrane, respectively, from $\mathcal{I} \times \mathcal{R}$ onto $\mathcal{R}$:

$$r(s, t) = R + w(s, t), \qquad x(s, t) = s + u(s, t). \tag{3}$$

At the same time, the place $p = p(s, \alpha, \varrho) \in \Omega$ is mapped into another position

$$\varphi_t(s, \alpha, \varrho) = o + x(s, t)\mathbf{e} + \frac{r(s, t)}{R}\varrho\mathbf{c}(\alpha); \tag{4}$$

the map φ_t describes the evolution of the area Ω, that is, the evolution of the region where the fluid flows. Obviously, (4) matches with the maps describing the evolution of the membrane in such a way that the image of $\varphi_t(s, \varrho, \alpha)$ coincide with $\mathcal{C}$ when $\varrho = R$.

2.1. The fluid flow model

The blood is modeled as an incompressible, linearly viscous fluid. Blood includes many rheological features that cannot be grasped by a linearly viscous fluid model; nevertheless, our aim is to find an averaged model, and the local viscous effect, such as recirculation sites, or higher shear rate, are deemed unimportant. The focus of this work is on the blood–vessel interaction versus

prestress effects and in this respect the use of a constant viscosity model is justified. Moreover, given the peculiar geometry of the problem we are interested in, we will derive a one-dimensional, cross-average model of the blood-flow from the following main assumptions (Quarteroni and Formaggia, 2003):

- fluid flow is axisymmetric;
- pressure is constant on each cross section of the tube-like region;
- only body forces of inertial type are considered.

Here, to match the fluid and the solid descriptions, and in contrast with the standard usages in fluid mechanics, we describe the fluid flow in a referential form, that is, using fields defined on particle points rather than of position, as proposed in (Di Carlo et al., 1999), where a detailed discussion on this topic can be found. Thus, we introduce the axisymmetric *reference velocity field*

$$(s,\varrho,\alpha,t)\mapsto \mathbf{v}(s,\varrho,\alpha,t)=v_a(s,\varrho,t)\mathbf{e}+v_r(s,\varrho,t)\mathbf{c}(\alpha), \tag{5}$$

giving the velocity possessed in time t by the fluid particle that at that time is in $\varphi_t(s,\varrho,\alpha)$. The axial component v_a of the velocity field is represented in terms of a profile function $f(\varrho)$ and of the mean axial velocity $v(s,t)$

$$v_a(s,\varrho,t)=f(\varrho)v(s,t),\quad v(s,t)=\frac{1}{A}\int_{\mathcal{L}} v_a(s,\varrho,t), \tag{6}$$

with A representing the area of the cross section $\mathcal{L}$; the radial component v_r is assumed to have null mean velocity. Moreover, as is usual, we introduce the momentum-flux correction (also known as Coriolis coefficient) β such that

$$Av^2\beta=\int_{\mathcal{L}} v_a^2. \tag{7}$$

2.1.1. The incompressibility condition

If ν denotes the usual spatial flow field, we have

$$\mathbf{v}(\cdot,t)=\nu\big(\varphi_t(\cdot),t\big);$$

then, the incompressibility condition prescribes that $\operatorname{Div}\nu=\mathbf{I}\cdot\operatorname{Grad}\boldsymbol{\nu}=0$. Introduced $\boldsymbol{\Phi}=\operatorname{Grad}\varphi_t$, it is a straightforward exercise to verify that the same incompressibility condition may be written in a referential form as

$$\operatorname{Grad}\mathbf{v}\cdot\Phi^{-T}=0. \tag{8}$$

In particular, given that the representation forms are (4) and (5), we find

$$\operatorname{Grad}\mathbf{v}=(v_a'\mathbf{e}+v_r'\mathbf{c})\otimes\mathbf{e}+\frac{1}{\varrho}v_r\mathbf{c}'\otimes\mathbf{c}'+(v_{a,\varrho}\mathbf{e}+v_{r,\varrho}\mathbf{c})\otimes\mathbf{c}, \tag{9}$$

$$\Phi^{-T}=\frac{1}{d}\hat{I}+\frac{1}{x'}\mathbf{e}\otimes\mathbf{e}-\frac{\varrho d'}{x'd}\mathbf{e}\otimes\mathbf{c},\quad d(s,t)=\frac{1}{R}r(s,t), \tag{10}$$

where the prime denotes the derivative with respect to the coordinate spanning the tube axis and $\hat{\mathbf{I}}=\mathbf{I}-\mathbf{e}\otimes\mathbf{e}$.[1] Thus, Eq. (8) assumes the form:

$$\frac{1}{x'}\left(v_a'-\frac{d'}{d}\varrho v_{a,\varrho}\right)+\frac{1}{d}\left(\frac{v_r}{\varrho}+v_{r,\varrho}\right)=0. \tag{11}$$

The 1-D cross-average incompressibility turns out by integrating Eq. (11) on the cross section $\mathcal{L}$ and accounting for the kinematic matching conditions between fluid and membrane:

$$v_a(s,R,t)=\dot{x}(s,t),\qquad v_r(s,R,t)=\dot{r}(s,t), \tag{12}$$

with a superposed dot denoting time derivative. It results

$$\dot{r}+\frac{1}{x'}\left(r'v+\frac{1}{2}rv'-r'\dot{x}\right)=0. \tag{13}$$

[1] Notice that, given two vectors $\mathbf{a},\mathbf{b}\in\mathcal{V}$, we define their tensor product $\mathbf{a}\otimes\mathbf{b}$ to be the linear mapping which acts on $\mathcal{V}$ as follows: for any $\mathbf{c}\in\mathcal{V}$, $(\mathbf{a}\otimes\mathbf{b})\mathbf{c}=(\mathbf{b}\cdot\mathbf{c})\mathbf{a}$.

2.1.2. The balance equation

The only relevant balance equation in our problem is the longitudinal one. To obtain the cross-average version of this equation, we first project the full 3D balance equation on the cylinder axis **e**; then, we integrate the resulting scalar equation on the cross section:

$$\int_{\mathcal{L}} \big((S\mathbf{e}\cdot\mathbf{e})' + d\cdot\mathbf{e}\big) + \int_{\partial\mathcal{L}} S\mathbf{c}\cdot\mathbf{e} = 0, \quad \text{on } (0,L);$$

$$\int_{\mathcal{L}} S\mathbf{e}\cdot\mathbf{e} = s_o, \quad \text{on } \{0\}, \qquad \int_{\mathcal{L}} S\mathbf{e}\cdot\mathbf{e} = -s_L, \quad \text{on } \{L\}. \tag{14}$$

The stress S and the inertial force d have the following constitutive prescriptions (Di Carlo et al., 1999)

$$S = \big(-pI + 2\mu\,\mathrm{sym}\big((\mathrm{Grad}\,\mathbf{v})\Phi^{-1}\big)\big)\Phi^{*}, \tag{15}$$

$$d = -\hat{\varrho}\big(\dot{\mathbf{v}} + (\mathrm{Grad}\,\mathbf{v})\Phi^{-1}(\mathbf{v} - \dot{\varphi}_t)\big), \tag{16}$$

where the scalar field p represents the transmural pressure, the scalar parameter μ is the viscosity, and $\hat{\varrho}$ the reference mass density. The second integral in the bulk balance equation accounts for the actions exerted on the fluid by the vessel wall, whereas s_0 and s_L represent the actions on the fluid at the inlet and outlet, respectively.

Using the incompressibility condition (13), the constitutive prescriptions (15)–(16), and under the aforementioned conditions assumed for the flow, the integrals of the bulk balance equation yield:

$$\int_{\mathcal{L}} (S\mathbf{e}\cdot\mathbf{e})' = \left(2\mu\frac{A}{x'}\big(d^2v' + 2\big(f(R)-1\big)dd'v\big) - Ad^2p\right)', \tag{17}$$

$$\int_{\mathcal{L}} d\cdot\mathbf{e} = -\hat{\varrho}A\left(\dot{v} - \frac{\dot{x}}{x'}v' + 2\frac{\beta}{x'}vv' + 2\big(f(R)-1\big)\left(\frac{r'\dot{x}}{rx'} - \frac{\dot{r}}{r}\right)v - 2\big(f^2(R)-\beta\big)\frac{r'v^2}{rx'} + 2\frac{\dot{r}}{r}f(R)v\right), \tag{18}$$

$$\int_{\partial\mathcal{L}} S\mathbf{c}\cdot\mathbf{e} = 2\mu\pi R\left(\left(\frac{R^2(d')^2}{x'} + x'\right)f'(R)v + \big(dv_r(R)\big)' - \frac{rdd'}{2x'}f(R)v'\right) + 2Add'p. \tag{19}$$

Standard additional assumptions (Quarteroni and Formaggia, 2003) are taken into account in order to obtain simpler equations, namely,

- the longitudinal velocity of the wall is considered to be null, $\dot{x} = 0$; thus, Eqs. $(6)_1$ and $(12)_1$ imply $f(R) = 0$;
- the velocity profile $f(\varrho)$ is assumed such to yield a momentum flux coefficient $\beta = 1$.

Thus, the reduced incompressibility and balance equations are

$$\dot{r} + \frac{1}{x'}\left(r'v + \frac{1}{2}rv'\right) = 0, \tag{20}$$

$$\hat{\varrho}\left(\dot{v} + \frac{1}{x'}vv'\right) = -\frac{r^2}{R^2}p' + 2\mu\frac{1}{R^2}\left(\left(\frac{(r^2v)'}{x'}\right)' + \frac{\delta^2}{x'}Rf'(R)v + (r\dot{r})'\right). \tag{21}$$

In the following, we shall disregard the viscosity term by setting $\mu = 0$. In major arteries the effect of the fluid viscosity in wave propagation phenomena is negligible (Fung, 1993): the flow is almost steady since the characteristic wavelenghts are much greater than the vessel radius. Our opinion is that fluid viscosity influences the local flow pattern, but does not influence the averaged model that we used.

As customary for pipe flow problems, the boundary conditions that we set concern inflow at the inlet and pressure at the outlet. For the problem we are considering here, such conditions are not known apriori and should be related to the presence of the remaining vascular bed. Among the many mathematical models of the systemic circulation proposed, we chose a discrete model which will be discussed in the following section.

2.2. The wall model

To deal with other main issue, which is to account for the compliance of the vessel and the prestress state of the artery walls, we modeled the vessel as an axisymmetric elastic membrane whose reference configuration may be stressed, and we proposed

a linearized incremental balance problem. Stresses in the reference configuration, which enter the problem as independent parameters, account for the in vivo conditions of large arteries; the small stresses due to the pulsatile blood pressure, the unknowns of the problem, sum up with the reference parameters.

A detailed presentation of the nonlinear model for the axisymmetric membrane, together with the linearized incremental problem can be found in Nardinocchi and Teresi (2003). We assume that the stress state of the reference configuration Ω is characterized by longitudinal and circumferential stresses T_1^o and T_2^o, respectively, balanced by a constant pressure field p_o and a traction F_o

$$RT_2^o = p_o, \qquad T_1^o = F_o. \tag{22}$$

Then, we introduce the parameters λ_1^o and λ_2^o, representing the longitudinal and circumferential stretches of the reference configuration with respect to a stress-free configuration.

Following Zhou and Fung (1997), we assume that the mechanical response of the membrane is well described by the following strain energy density function

$$\sigma(\lambda_1, \lambda_2) = \frac{c}{2}\big(\mathrm{e}^{Q(\lambda_1,\lambda_2)} - 1\big), \tag{23}$$

$$Q(\lambda_1, \lambda_2) = b_1\big(E_1(\lambda_1)\big)^2 + 2b_4 E_1(\lambda_1)E_2(\lambda_2) + b_2\big(E_2(\lambda_2)\big)^2, \quad E_\alpha(\lambda_\alpha) = \frac{1}{2}\big(\lambda_\alpha^2 - 1\big),\ \alpha = 1, 2, \tag{24}$$

where λ_1 and λ_2 measure the longitudinal and circumferential stretches, respectively, of the current configuration with respect to the stress-free state, c is a material constant ($[c] = Nm^{-1}$) and b_1, b_2, and b_4 are nondimensional constants. The values of the constants can be inferred by experimental tests. Here we use a data set coming from tests on the canine thoracic aorta (Zhou and Fung, 1997). The Cauchy stresses T_1 and T_2 corresponding to the function (23)–(24) are

$$T_1 = \widehat{T}_1(\lambda_1, \lambda_2) = \frac{1}{\lambda_2}\frac{\partial\sigma}{\partial\lambda_1} = c\frac{\lambda_1}{\lambda_2}(b_1E_1 + b_4E_2)\exp(Q), \tag{25}$$

$$T_2 = \widehat{T}_2(\lambda_1, \lambda_2) = \frac{1}{\lambda_1}\frac{\partial\sigma}{\partial\lambda_2} = c\frac{\lambda_2}{\lambda_1}(b_4E_1 + b_2E_2)\exp(Q). \tag{26}$$

In the following analysis, we assume the stretches $(\lambda_1^o, \lambda_2^o)$ as assigned parameters and study the small motions from the reference configuration. Let us note that, once the stretches $(\lambda_1^o, \lambda_2^o)$ are fixed, by using Eqs. (25)–(26), we obtain the reference stresses

$$T_1^o = \widehat{T}_1(\lambda_1^o, \lambda_2^o), \qquad T_2^o = \widehat{T}_2(\lambda_1^o, \lambda_2^o), \tag{27}$$

and from these latter, through Eqs. (22), the corresponding reference loads p_o, F_o.

Therefore, when u and w are small enough, the longitudinal and circumferential stretches at the present configuration are given by

$$\lambda_1 = (1 + u')\lambda_1^o, \qquad \lambda_2 = (1 + w/R)\lambda_2^o. \tag{28}$$

Using (28), we can linearize the constitutive relation (25) and (26) around the reference stress state T_1^o, T_2^o, obtaining the linearized constitutive laws relating the stresses T_1 and T_2 to u' and w/R

$$T_1 = \big(T_1^o + D_{11}(\lambda_1^o, \lambda_2^o)\big)u' + \big(-T_1^o + D_{12}(\lambda_1^o, \lambda_2^o)\big)\frac{w}{R}, \tag{29}$$

$$T_2 = \big(-T_2^o + D_{21}(\lambda_1^o, \lambda_2^o)\big)u' + \big(T_2^o + D_{22}(\lambda_1^o, \lambda_2^o)\big)\frac{w}{R}, \tag{30}$$

with

$$D_{11}(\lambda_1^o, \lambda_2^o) = c\frac{(\lambda_1^o)^3}{\lambda_2^o}\big(b_1 + 2(b_1E_1^o + b_4E_2^o)^2\big)\exp(Q_o),$$

$$D_{22}(\lambda_1^o, \lambda_2^o) = c\frac{(\lambda_2^o)^3}{\lambda_1^o}\big(b_2 + 2(b_4E_1^o + b_2E_2^o)^2\big)\exp(Q_o), \tag{31}$$

and

$$D_{12}(\lambda_1^o, \lambda_2^o) = D_{21}(\lambda_1^o, \lambda_2^o) = c\lambda_1^o\lambda_2^o\big(b_4 + 2(b_1E_1^o + b_4E_2^o)(b_4E_1^o + b_2E_2^o)\big)\exp(Q_o). \tag{32}$$

The *linear* constitutive laws (29), (30) depend *nonlinearly* on the stretches λ_1^o and λ_2^o; moreover, for $\lambda_1^o = \lambda_2^o = 1$ (that is, the reference configuration is stress and strain free) they reduce to the standard linear constitutive relations of an anisotropic membrane.

The balance equations for the membrane, linearized with respect to the stressed configuration, are

$$-T_1^o w'' + \frac{1}{R}(-T_2^o + D_{21}^o)u' + D_{22}^o \frac{w}{R^2} = b_r - \varrho \ddot{w}, \tag{33}$$

$$(T_1^o + D_{11}^o)u'' + (-T_2^o + D_{12}^o)\frac{w'}{R} = -b_s + \varrho \ddot{u}, \tag{34}$$

are valid for any $s \in (0, L)$. Here, b_r and b_s are the radial and longitudinal actions exerted by the blood on the vessel wall, respectively, and $D_{\alpha\beta}^o = D_{\alpha\beta}(\lambda_1^o, \lambda_2^o)$, $\alpha, \beta = 1, 2$.

Together with these bulk equations, we could have a boundary (balance) condition for the longitudinal stress T_1 in $s = 0$ and/or $s = L$.

3. Governing equations and boundary conditions

The blood–vessel interaction model we propose consists of Eqs. (20) and (21) for blood flow, and of Eqs. (33), (34) for the vessel. We assume the pressure field to be the sum of the constant term p_o plus a varying one $\tilde{p}$, representing addition of the pulsatile pressure of the blood flow. This, together with the small amount of the membrane displacements fields, yields a simplification in the pressure term of the fluid balance law

$$-\frac{r^2}{R^2}p' = -\frac{(R+w)^2}{R^2}(p_o + \tilde{p})' = -\tilde{p}'.$$

Moreover, being interested in phenomena for which the blood viscosity and the inertia of the arterial wall have minor effects, in the following it is assumed $\mu = 0$, $\ddot{u} = 0$, and $\ddot{w} = 0$; then, the actions exerted by the blood on the vessel wall reduce to $b_r = \tilde{p}$ and $b_s = 0$, and we must solve the problem represented by the following equations:

$$\dot{r} + \frac{1}{x'}\left(r'v + \frac{1}{2}rv'\right) = 0, \quad r = R + w, \quad x' = 1 + u', \tag{35}$$

$$\hat{\varrho}\left(\dot{v} + \frac{1}{x'}vv'\right) = -\tilde{p}', \tag{36}$$

$$-T_1^o w'' + \frac{1}{R}(-T_2^o + D_{21}^o)u' + D_{22}^o \frac{w}{R^2} = \tilde{p}, \tag{37}$$

$$(T_1^o + D_{11}^o)u'' + (-T_2^o + D_{12}^o)\frac{w'}{R} = 0, \tag{38}$$

where the unknown fields are the displacements w and u of the wall, the velocity v and the pressure $\tilde{p}$ of the fluid. It is worth noting that the system (35)–(38) describes small motions of the membrane due to the blood pressure pulsating of a small amount $\tilde{p}$ around a mean, although high, pressure p_o, but no hypothesis on the smallness of v has been done, and the fluid balance equation (36) remains nonlinear with respect to v.

The above system of differential equations models flow and wall dynamics in a finite arterial segment, and has to be equipped with appropriate boundary conditions. For the vessel, we assume that at both the ends the radial displacement of the wall is related to the pressure and that the axial displacement is null:

$$D_{22}^0 w = \tilde{p}R^2, \quad u = 0 \quad \text{in } \{0\}, \{L\}. \tag{39}$$

For the fluid flow, we chose as boundary conditions the upstream pressure $p_u = \tilde{p}(0)$ and the downstream flow rate $Q_d = v(L)A(L)$, but we do not assign them explicitly. We considered a closed-loop system that couples two different models: a fine one, the continuum model described above, which deals with the finite arterial segment, and a rougher one that accounts for the systemic circulation.

Many simplified models of the closed-loop cardiovascular system are available in literature. Here we chose those which mimic electrical circuits, for which flow rate and pressure have the role of current and voltage. The whole vascular tree is modelled as a closed network, whose behaviour is characterized by a set of given parameters R_k, C_k, L_k such as resistance, compliance and inductance, each of them labelled with an index k and whose state is represented by the pair flow rate and pressure at each node (see Avanzolini et al., 1988; Ottesen et al., 2004). Among the many adjectives used to label these models, as *lumped* or *zero-dimensional*, here we shall refer to them as *discrete* models to highlight the dichotomy with the continuum models.

Here, we used the network proposed by Avanzolini et al. (1988) consisting of six sections for the circulatory system, plus another which represent the *ventricle* pumps (see Fig. 2). The balance laws of the network yield the following system of time dependent ordinary differential equations:

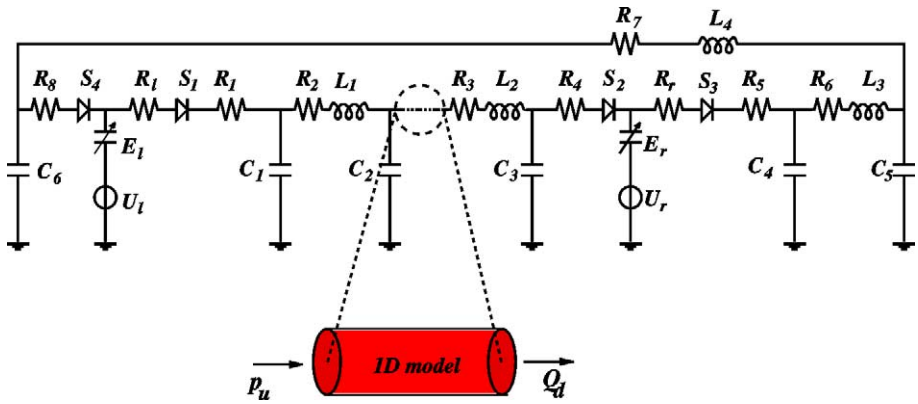

Fig. 1. Insertion of the continuum model in the discrete one. The vascular compartments are connected to form a closed loop, in analogy with electrical circuits. Pressure and flow data of the network become the boundary conditions for the continuum model (by courtesy of Formaggia et al., 1999).

$$
\begin{aligned}
&C_1\dot{x}_1 = s_1 z_1/(R_l + R_1) - x_2,\\
&L_1\dot{x}_2 = x_1 - R_2 x_2 - x_3,\\
&C_2\dot{x}_3 = x_2 - x_4,\\
&L_2\dot{x}_4 = x_3 - R_3 x_4 - x_5,\\
&C_3\dot{x}_5 = x_4 - s_2 z_2/R_4,\\
&\dot{x}_6 = s_2 z_2/R_4 - s_3 z_3/(R_r + R_5),\\
&C_4\dot{x}_7 = s_3 z_3/(R_r + R_5) - x_8,\\
&L_3\dot{x}_8 = x_7 - R_6 x_8 - x_9,\\
&C_5\dot{x}_9 = x_8 - x_{10},\\
&L_4\dot{x}_{10} = x_9 - R_7 x_{10} - x_{11},\\
&C_6\dot{x}_{11} = x_{10} - s_4 z_4/R_8,\\
&\dot{x}_{12} = s_4 z_4/R_8 - s_1 z_1/(R_1 + R_l).
\end{aligned}
\tag{40}
$$

The system describes the time evolution of a discrete set of values of flow rate and pressure, that represent mean values of different compartments: x_i for $i = 1, 3, 5, 7, 9, 11$ indicate pressure, for $i = 2, 4, 8, 10$ the flow rates; the pair x_6, x_{12} denotes the volume variation in the right and the left ventricle, respectively, as compared to a reference volume. Finally, the variables s_i $(i = 1, 4)$ represent the state of two diodes simulating the cardiac valves and are such that:

$$
s_i = \begin{cases} 1, & z_i > 0,\\ 0, & z_i < 0, \end{cases}
$$

depending on the sign of pressure gradient z_i $(i = 1, 4)$ at their ends. The cardiac activity is modelled through the assignement of a given function $P_v(t)$, inferred by linearizing the pressure-flow relation concerning the systolic and diastolic phases (see Avanzolini et al., 1988, for further details).

The rough model described here and the finer one presented in previous sections can be coupled using the following strategy. We insert another node in the discrete model, and relate the two new state variables of the added node with the boundary conditions of the continuum model. Moreover, we allow for the development of the evolution of the new variables to be ruled implicitly by the PDE system (35)–(38).

Following Formaggia et al. (1999) we add a node at the point shown in Fig. 1, corresponding to the descending aorta. Then, we identify the two additional state variables with the upstream flow rate $Q_u = v(0)A(0)$ and the downstream pressure $p_d = \tilde{p}(L)$. Meanwhile, the upstream pressure p_u is identified with x_3, and the downstream flow rate Q_d with x_4. Accordingly, everywhere in the discrete model we have the substitution

$$
x_3 \mapsto p_u, \qquad x_4 \mapsto Q_d; \tag{41}
$$

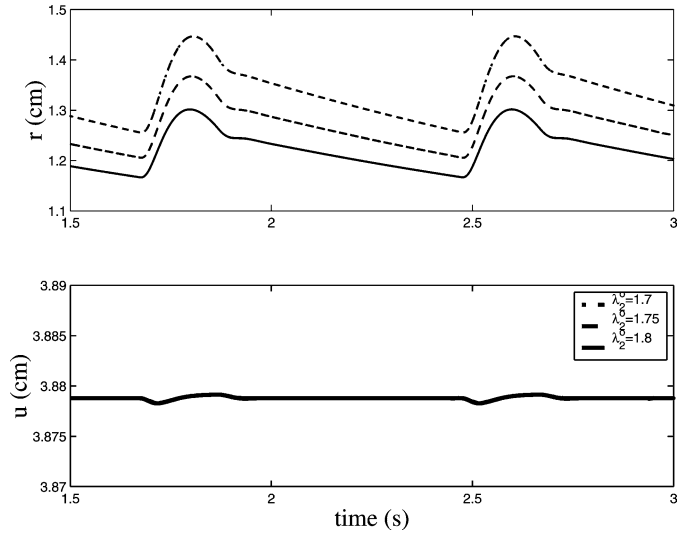

Fig. 2. Time histories of $r = R + w$ and $u = x - s$ at the center of the vessel ($s = L/2$) for three values of the circumferential prestress (for $\lambda_1^o = 1.4$ fixed).

moreover, to account for the added node, Eqs. $(40)_3$, $(40)_4$ are replaced by:

$$C_2 \dot{p}_u = x_2 - Q_u, \tag{42}$$

$$L_2 \dot{Q}_d = p_d - R_3 Q_d - x_5. \tag{43}$$

Eventually, we have two coupled models that consist in a unique closed-loop system, and the fine model is implicitly provided with boundary conditions that reproduce the proper waveforms entering the vessel and avoid spurious reflections (Pontrelli, 2004).

4. Numerical results

We are obliged to solve the PDE problem (35)–(38), with the boundary conditions (39), together with the ODE system (40), with the substitutions (41), (42) and (43).

We use the following values for the continuum model:[2]

$$c = 2 \cdot 10^5 \text{ dyne/cm}, \quad c_1 = 0.38, \quad c_2 = 0.26, \quad c_3 = 0.046,$$
$$R = 1.2 \text{ cm}, \quad L = 8 \text{ cm}, \quad \hat{\rho} = 1.05 \text{ g/cm}^3;$$

while the discrete value has the same numerical parameters as in Pontrelli (2004).

The PDE system is solved using a staggered grid technique. We divide the domain $(0, L)$ with $n + 1$ equispaced points x_i, $i = 0, \ldots, n$, on which the main fields are computed; then, we use n intermediate nodes at $x = (x_i + x_{i+1})/2$ to evaluate membrane strains and stresses.

Time integration is performed using a second order Runge–Kutta scheme for both the systems. In order to guarantee numerical stability and independence from discretization, we use grid intervals with length $\Delta x = 0.01$ cm, and a time step $\Delta t = 10^{-4}$ s. A brief sketch of the algorithm follows

- Updating from instant t^k to $t^{k+1} = t^k + \Delta t$:
  the state $x_i(t^k)$ of the discrete system is known: we use the values $x_3(t^k) = p_u$ and $x_4(t^k) = Q_d$ as flow boundary conditions to solve the PDE problem; thus, knowing the solution, we compute $Q_u(t^k)$ and $p_d(t^k)$. The right-hand term of the ODE system is now completely known at $t = t^k$ and we can integrate it. We can update $x_i(t^k)$ to $x_i(t^{k+1})$.

[2] Note that c in (23) is obtained by integration across the wall thickness of the analogous density energy function in Zhou and Fung (1997).

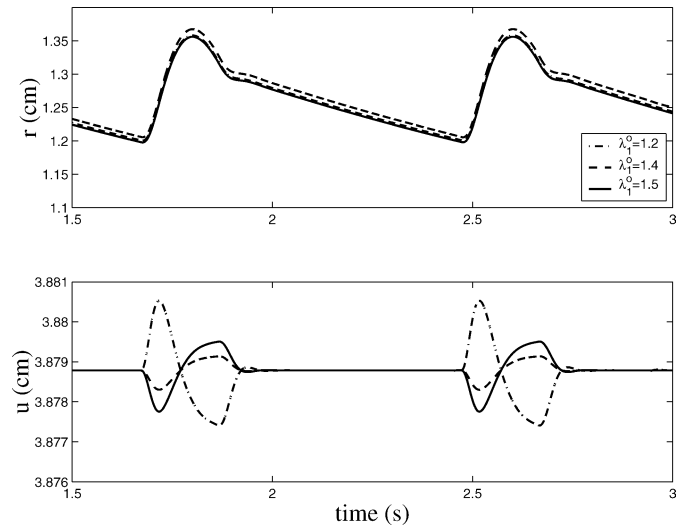

Fig. 3. Time histories for $r = R + w$ and $u = x - s$ at the center of the vessel ($s = L/2$) for three values of the longitudinal prestress (for $\lambda_2^o = 1.75$ fixed).

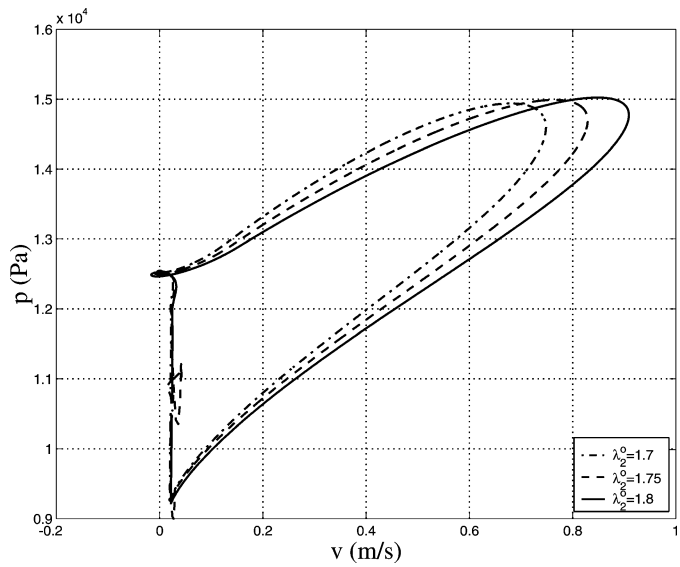

Fig. 4. PV loop curves at the center of the vessel ($s = L/2$) for $\lambda_1^o = 1.4$.

- The start up:
  we assign an initial guess for the values $x_i(0)$ of the ODE system; then, we repeat the updating procedure until the initial state stabilizes.

The goal of this numerical investigation is to analyze the dependence of the smaller displacements u and w of the membrane and of the flow variables v and $\tilde{p}$ on the assigned prestessed states, parametrized by the stretches λ_1^o and λ_2^o characterizing the stretch state of the reference configuration of the vessel. It has been observed that, under the pulsatile blood pressure (governed by the parameter setting in the discrete model), the wall expands and begins to oscillate periodically in time around a mean value. As evident from Eqs. (29) and (30), the relation between the small elastic deformations u' and w/R and the stresses T_1 and T_2 is anisotropic both from the elastic and geometric point of view. Thus, longitudinal and circumferential reference stretches affect the response of the vessel differently. In particular, the radial displacement w is much more sensitive to the stretch λ_2^o than to λ_1^o.

In Fig. 2, the behaviour of the fields $r = R + w$ and $x = s + u$ is shown in correspondence to three different values of the parameters λ_2^o (with λ_1^o fixed); Fig. 3 shows the analogous behavior in correspondence to three different values of λ_1^o (with λ_2^o fixed). In both the figures, the fields $r = R + w$ and $x = s + u$ are evaluated at $s = L/2$ (the center of the vessel).

Our results show that the vessel displacements are sensitive to the reference stretches, but their dependence on $(\lambda_1^o, \lambda_2^o)$ is very different. The radius $r = R + w$ strongly depends upon the circumferential reference stretch. In particular, it decreases monotonically with λ_2^o. The same radius is less sensitive to the longitudinal stretch and, more importantly, when λ_1^o increases, it attains a maximun and then decreases. The longitudinal displacements are less affected by the variation of the reference stretches and $x = s + u$ is much more sensitive to λ_1^o than to λ_2^o.

As far as the flow variables $\tilde{p}$ and v are concerned, only minor changes have been observed in the values they attain, but the phase velocity of pressure waves shows a noteworthy sensitivity to reference stretches. The phase velocities can be measured by way of the method suggested in Khir and Parker (2002) by measuring the slopes of the PV-loop curves, that is to say, the curves parametrized with time in the pressure-velocity plane. For a typical PV loop, as in Fig. 4, the phase velocity is in agreement with the physiological values; at the center of the vessel, the velocity varies between 3.8 m/s and 5 m/s, depending upon the value of prestress λ_2^o.

5. Conclusions

Mathematical models aimed at predicting wave propagation characteristics for arterial vessels – such as velocity and impedance – may be of clinical interest. The outcome of such efforts is to give physiological indicators of diagnostic significance and to detect anomalies that could be used to address pathological states in the vascular system.

The technique we propose is capable of predicting gross propagation features, that will have relevant significance, with a modest computational effort.

The behaviour of compliance vessels conveing blood flow has been studied in relation to the elastic nonlinear properties of the vessel wall and to the presence of high prestress states. The mechanical blood–vessel interaction is described by a one-dimensional continuum model and is expressed by a set of four nonlinear partial differential equations. The hyperbolic nature of the propagation phenomenon has been analyzed in the linearized case.

To account for global circulation features, the continuum model has been coupled with a comprehensive discrete model which provides the proper boundary conditions by reproducing the correct waveforms entering the vessel and avoid unphysical reflections at the outlet. This constitutes an improvement of the previous studies where a simple Windkessel model has been used to approximate the arterial termination.

For its multiscale structure, the present model depends on many physical, geometrical and material parameters. To discriminate among them, the emphasis has been put on the wall elasticity, that greatly affects the wave propagation. On the other hand, the fluid viscosity has been disregarded because of its small influence.

The model has some limitations: one is due to the mechanics of the wall, approximated as a thin shell with negligible inertia and no bending stiffness. Nevertheless, by including the longitudinal deformation, it reproduce the waveforms and the pressure pulse quite well, and offers a predictive insight in propagation phenomena. The model is adaptable for variable elastic properties of the vessel and could be used to analyze the modified flow and structure pattern consequent to a prosthetic insertion. Actually, we plan to apply such a technique to study the effect of local narrowing and stiffening of the artery on the flow and the wave propagation patterns.

Numerical simulations have focused on the effect of the elastic properties on the flow and on the wall deformations and the results, within a limited range of parameters, agree with physiological measurements with a good level of accuracy. The solution turns out to be much sensitive to the parameters of both the continuum and the discrete models and a more realistic estimate of them should be done on the basis on experiments and clinical data. The numerical algorithm allows us to discuss some results just for a precise class of initial state; so, the next step will consist in improving such an algorithm so to avoid such limits.

Finally, the geometrical, physical and biomechanical parameters need to be carefully identified according to a specific flow problem.

References

Atabek, H.B., Lew, H.S., 1966. Wave propagation through a viscous incompressible fluid contained in an initially stressed elastic tube. Biophysical J. 6, 481–503.

Avanzolini, G., Barbini, P., Cappello, A., Cevenini, G., 1988. CADCS simulation of the closed-loop cardiovascular system. Int. J. Biomed. Comput. 22, 39–49.

Di Carlo, A., Nardinocchi, P., Teresi, L., 1999. How to model blood flow in distensible vessels. In: Proceedings of the Third International Conference on Engineering Aero-HydroElasticity, Prague, 141–145.

Formaggia, L., Nobile, F., Quarteroni, A., Veneziani, A., 1999. Multiscale modelling of the circulatory system: a preliminary analysis. Comput. Visual Sci. 2, 75–83.

Fung, Y.C., 1993. Biomechanics. Mechanical Properties of Living Tissues. Springer.

Holzapfel, G.A., Gasser, T.C., Ogden, R.W., 2000. A new constitutive framework for arterial wall mechanics and a comparative study of material models. J. Elasticity 61, 1–48.

Holzapfel, G.A., Ogden, R.W. (Eds.), 2003. Biomechanics of Soft Tissue in Cardiovascular Systems. CISM Courses and Lectures, vol. 441. Springer.

Khir, A.W., Parker, K.H., 2002. Measurements of wave speed and reflected waves in elastic tubes and bifurcations. J. Biomech. 35, 775–783.

Kuiken, G.D.C., 1984. Wave propagation in a thin-walled liquid-filled, initially stressed tube. J. Fluid Mech. 141, 289–308.

Nardinocchi, P., Teresi, L., 2003. The influence of initial stresses on blood vessel mechanics. J. Mech. Mech. Biol. 3 (2), 215–229.

Ottesen, J.T., Olufsen, M.S., Larsen, J.K., 2004. Applied Mathematical Models in Human Physiology. SIAM Monograph on Math. Model & Comput.

Pontrelli, G., 2000. Blood flow through a circular pipe with an impulsive pressure gradient. Math. Models Methods Appl. Sci. 10, 187–202.

Pontrelli, G., 2004. A multiscale approach for modelling wave propagation in an arterial segment. Comput. Methods Biomech. Biomed. Engrg. 7, 79–89.

Quarteroni, A., 2001. Fluid–structure interaction for blood flow problems. In: Lecture Notes, AMS-AMIF Summer School, Prague, Czech Republic.

Quarteroni, A., Formaggia, L., 2003. Mathematical modelling and numerical simulation of the cardiovascular system. In: Ayache, N. (Ed.), Modelling of Living Systems. In: Ciarlet, P.G., Lions, J.L. (Eds.), Handbook od Numerical Analysis Series.

Sherwin, S.J., Formaggia, L., Peiro, J., Franke, V., 2003. Computational modelling of 1D blood flow with variable mechanical properties and its application to the simulation of wave propagation in the human arterial system. Int. J. Numer. Meth. Fluids 43 (6/7), 673–700.

Zhou, J., Fung, Y.C., 1997. The degree of nonlinearity and anisotropy of blood vessel elasticity. Proc. Natl. Acad. Sci. USA 94, 14255–14260.